Laboratory astrophysics and interstellar ices

G. Féraud[1], R. Basalgète[1], R. Dupuy[1], D. Torrez-Diaz[3], C. Romanzin[2], X. Michaut[1], P. Jeseck[1], L. Philippe[1], L. Amiaud[3], A. Lafosse[3], J-H. Fillion[1] et M. Bertin[1]

[1] LERMA, Sorbonne Univ. Observatoire de Paris, Paris, France
[2] ICP, Univ Paris Saclay, CNRS, Orsay, France
[3] ISMO, Univ Paris Saclay, CNRS, Orsay, France

PCMI 2022 - Paris

Processing of interstellar ices

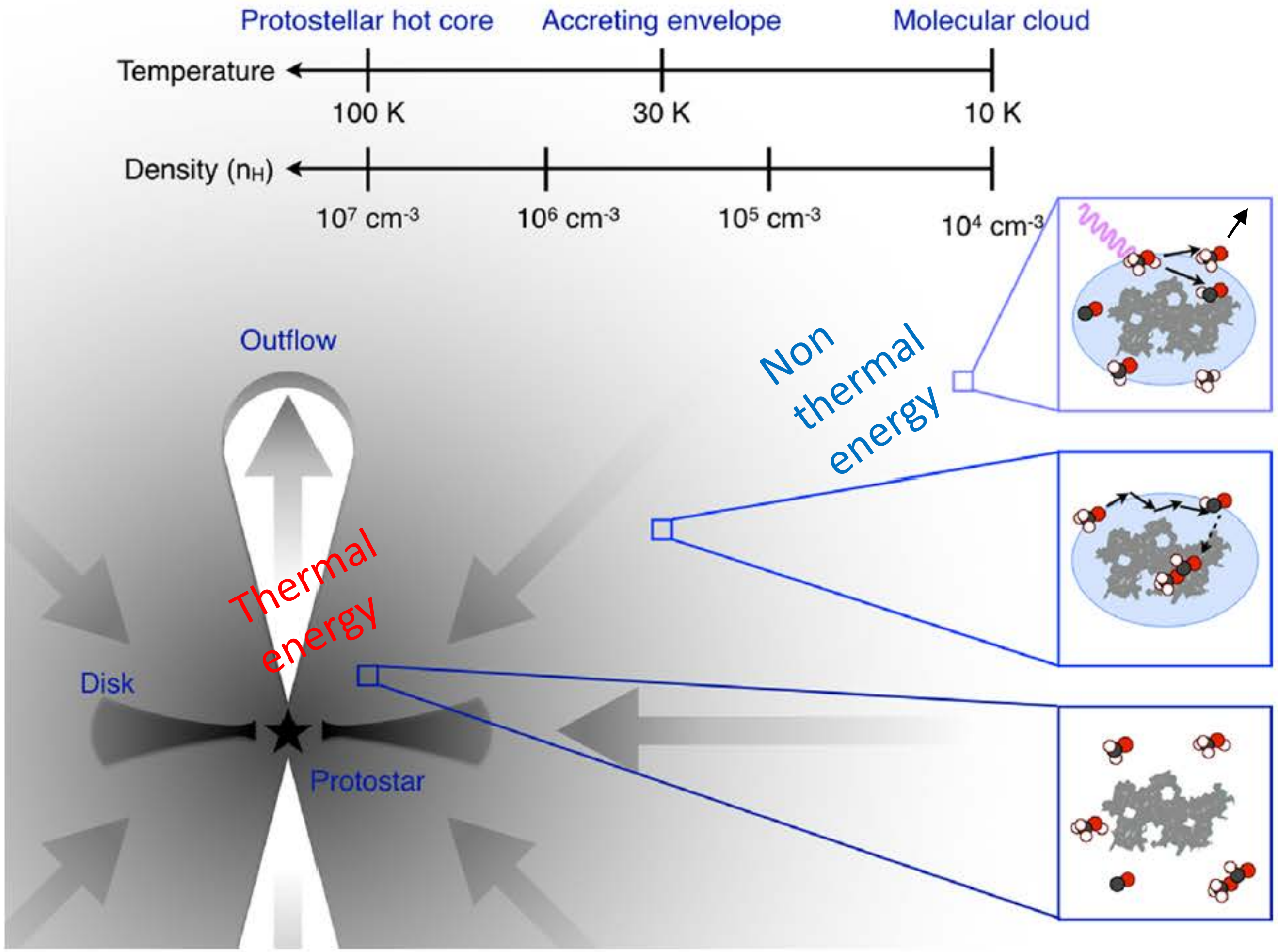

Figure 5. Cartoon of complex organic molecule formation through ice photochemistry during star formation. Simple ices form from atom addition reactions at low temperatures in dense molecular clouds. When these ices are exposed to UV radiation, some portion of the original ice is dissociated into radicals. As the icy grain heats up during star formation, the radicals become mobile and can combine to form more complex species. Some radical chemistry may also be possible in the coldest regions dependent on radical concentration and the efficiency of nonthermal diffusion.

Oberg 2016

Processing of interstellar ices – Non thermal energy sources

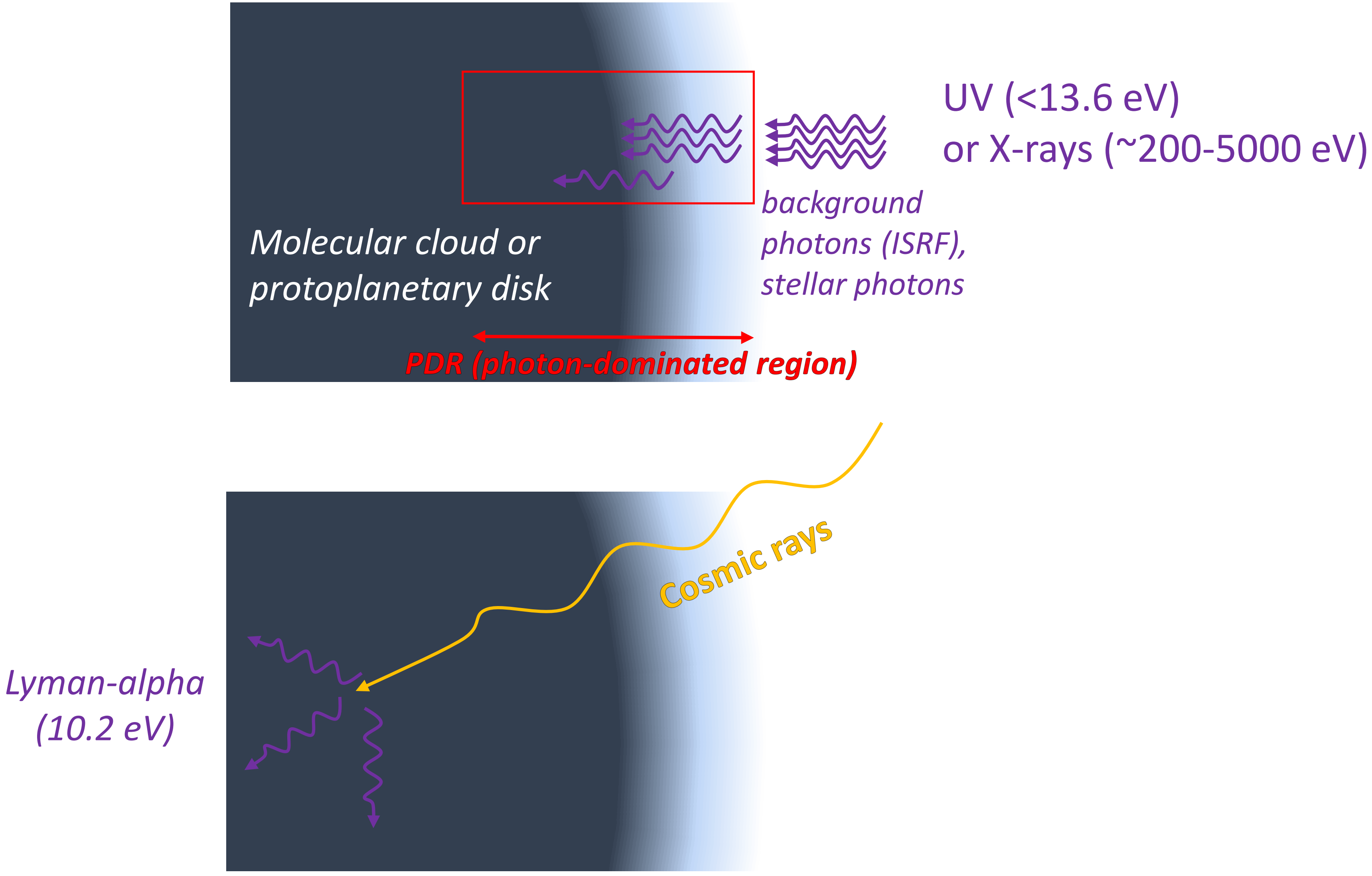

(Picture from M. Bertin)

Processing of interstellar ices – Some resolved observations

Hot core

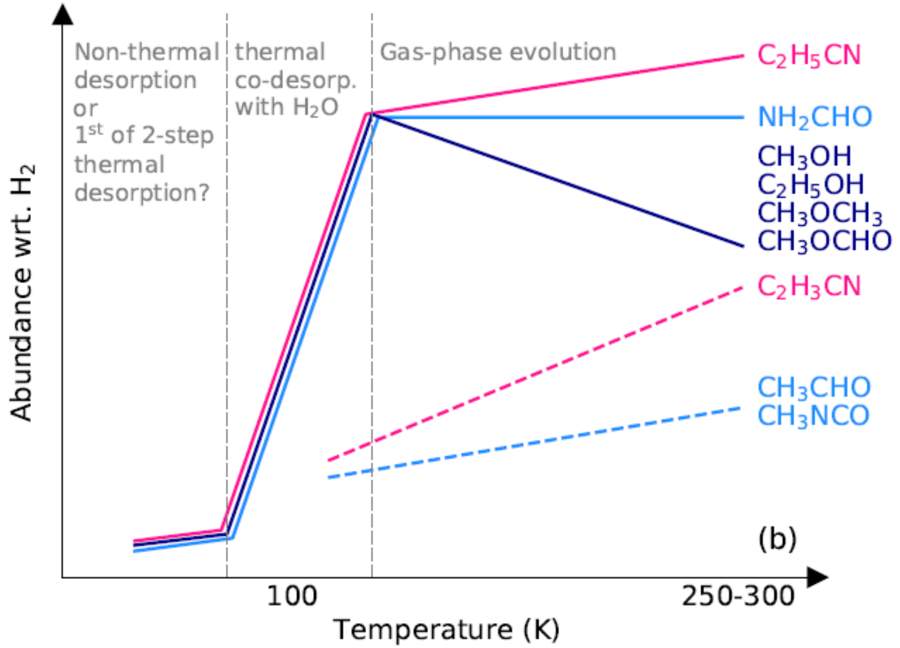

Busch+ 2022

COMs observations (ALMA) in a hot core

Protoplanetary Disk

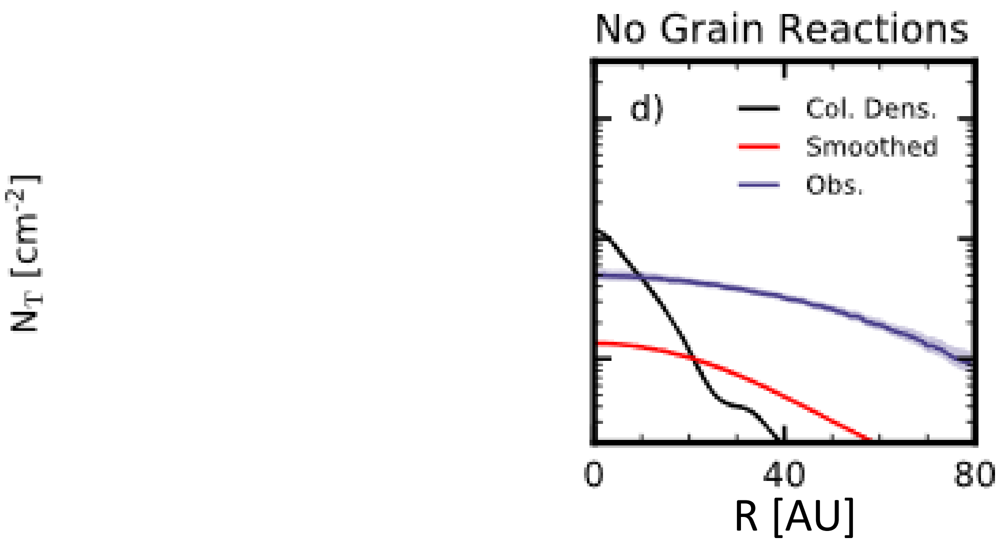

Loomis+2018

Figure 7. Panels (a, b): CH_3CN gas-phase abundances with grain-surface reactions turned on and off in the model, respectively. Temperature contours of 30 and 50 K are overlaid in black. Panels (c, d): CH_3CN gas-phase column densities for the abundance profiles shown in panels (a) and (b), respectively. Column density profiles smoothed with the synthesized beam are overplotted in red, and the observed column density profile from Figure 5 is overplotted in blue.

Photo-dissociation Region PDR

Guzman+ 2011, IRAM-30 m observations

(Simplified) Laboratory experiments on ices

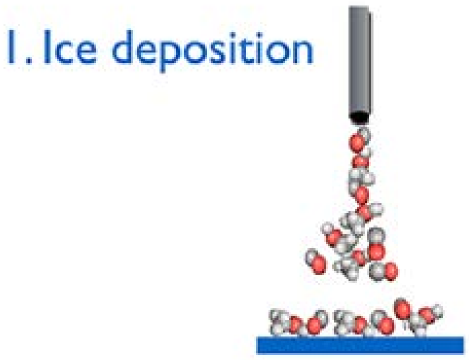

Sticking to a substrate See Philippe Parent's talk

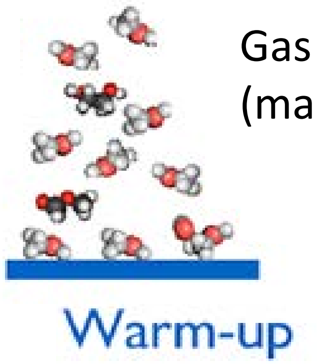

Gas phase detection (mass spectrometry)

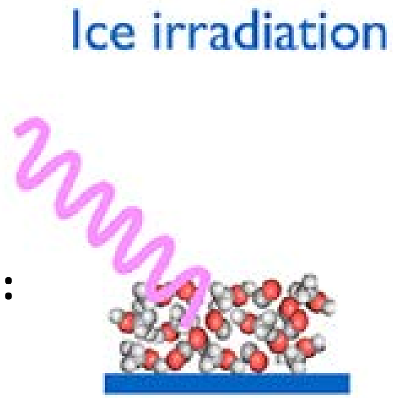

Photons :
Lasers
Lamp
Synchrotron
Cosmic Rays :
Accelerated Ions

Gas phase detection (mass spectrometry, chromatography)

Solid phase probes (Infrared, Electron paramagnetic resonance (EPR)...)

Laboratory data +/- close to astrophysical conditions

Astrochemical models

Adapted from Oberg 2016

Physico-chemical processes on/in ices

Thermal Energy

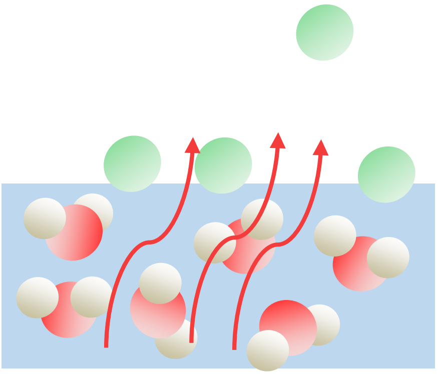

Thermal desorption

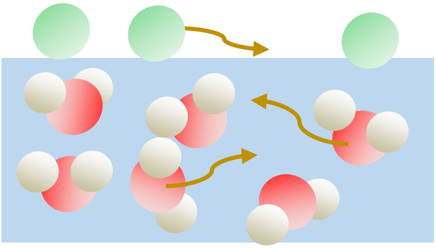

Diffusion

Non thermal Energy

dissociation and chemistry

Desorption after photon/CR irradiation or chemical reaction

Minissale+ 2016

Thermal Energy - Desorption

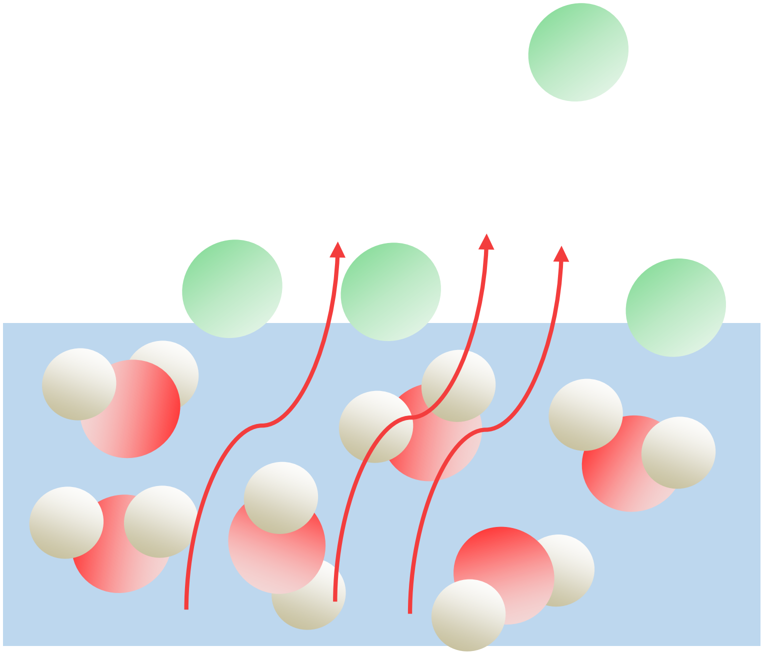

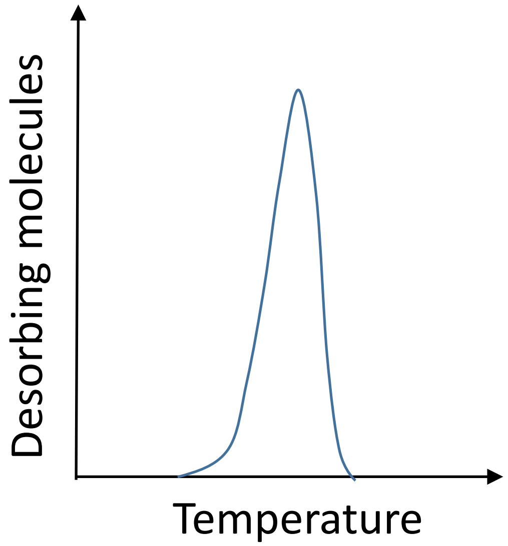

Temperature-programmed Desorption

- to determine snowlines location
- interpret astronomical observations
- build realistic and predictive astrochemical models.

See Franciele Kruczkiewicz's poster

Thermal Energy – Desorption

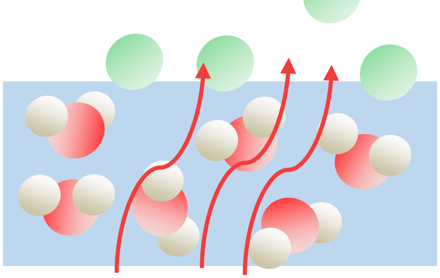

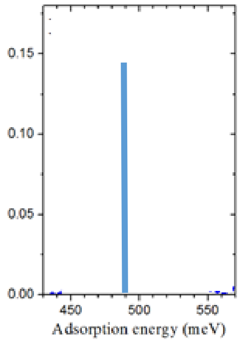

Review on thermal desorption
Minissale+2022

$$k_{\mathrm{td},i} \simeq \nu_i \, e^{-E_{\mathrm{b},i}/(k_\mathrm{B} T_\mathrm{s})}$$

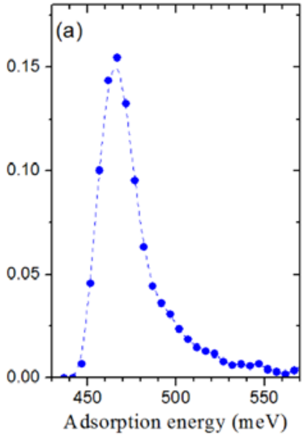

Doronin+2015

Table 2. Binding Energies of Sub-monolayer Regimes on Compact ASW[a]

	literature values						recommended values		
species	ν	E_{10}	E_{mode}	E_{90}	$E_{mean} \pm \Delta E$	ref	ν	E	T_{peak} (K)
H_2	10^{13}	300	450	600		25, 211−213	1.98×10^{11}	371	20
H	10^{12}	255		700		43−45, 213, 217, 218, 221	1.54×10^{11}	450	15
N	10^{12}	640	720	880		39	1.17×10^{13}	806	35
N_2	$10^{13}/4.1 \times 10^{15}$	970		1350	1152 ± 50	103	4.51×10^{14}	1074	35
O_2	5.4×10^{14}				1104 ± 55	103, 206	5.98×10^{14}	1107	35
CH_4	9.8×10^{14}				1368 ± 68	103	5.43×10^{13}	1232	47
CO	7.1×10^{11}	960	1140	1310		206	9.14×10^{14}	1390	35
O	10^{12}	1300		1700	1586 ± 480	39, 116, 208	2.73×10^{13}	1751	50
C_2H_2	3×10^{16}				3000 ± 220	227	4.99×10^{15}	2877	70
CO_2	$9.3 \times 10^{11}/3.0 \times 10^{7b}$	2236	2300	2346	2105 ± 902	116, 206, 229	6.81×10^{16}	3196	80
H_2S	10^{12}				2700	116, 166, 231	4.95×10^{15}	3426	85
H_2CO	10^{13}				3260	232	8.29×10^{16}	4117	95
CS	10^{12}				3200	116	6.65×10^{16}	4199	90
HCN	10^{12}				3700	116, 233	1.63×10^{17}	5344	137
NH_3	10^{12}				4600	116, 165, 234	1.94×10^{15}	5362	105
OH	10^{12}				4600	120, 235, 236	3.76×10^{15}	5698	140
H_2O	3.26×10^{15}				5640	187, 230, 237	4.96×10^{15}	5705	155
CH_3CN	10^{17}	5802	6150	6383		238, 239	2.37×10^{17}	6253	120
CH_3OH	10^{12}				5000	116	3.18×10^{17}	6621	128
NH_2CHO	10^{12}				6900	116, 209, 241	3.69×10^{18}	9561	176
C	10^{12}				14300	147	7.38×10^{14}	15 981	300

[a] ν in s^{-1} and E in K. The selected species are listed in ascending order of E value. See text for the choice of the preferred value. [b] Order of desorption is 1.07.

Thermal Energy – Desorption

Uncertainties in the binding energies => massive change in the ice abundances and profiles

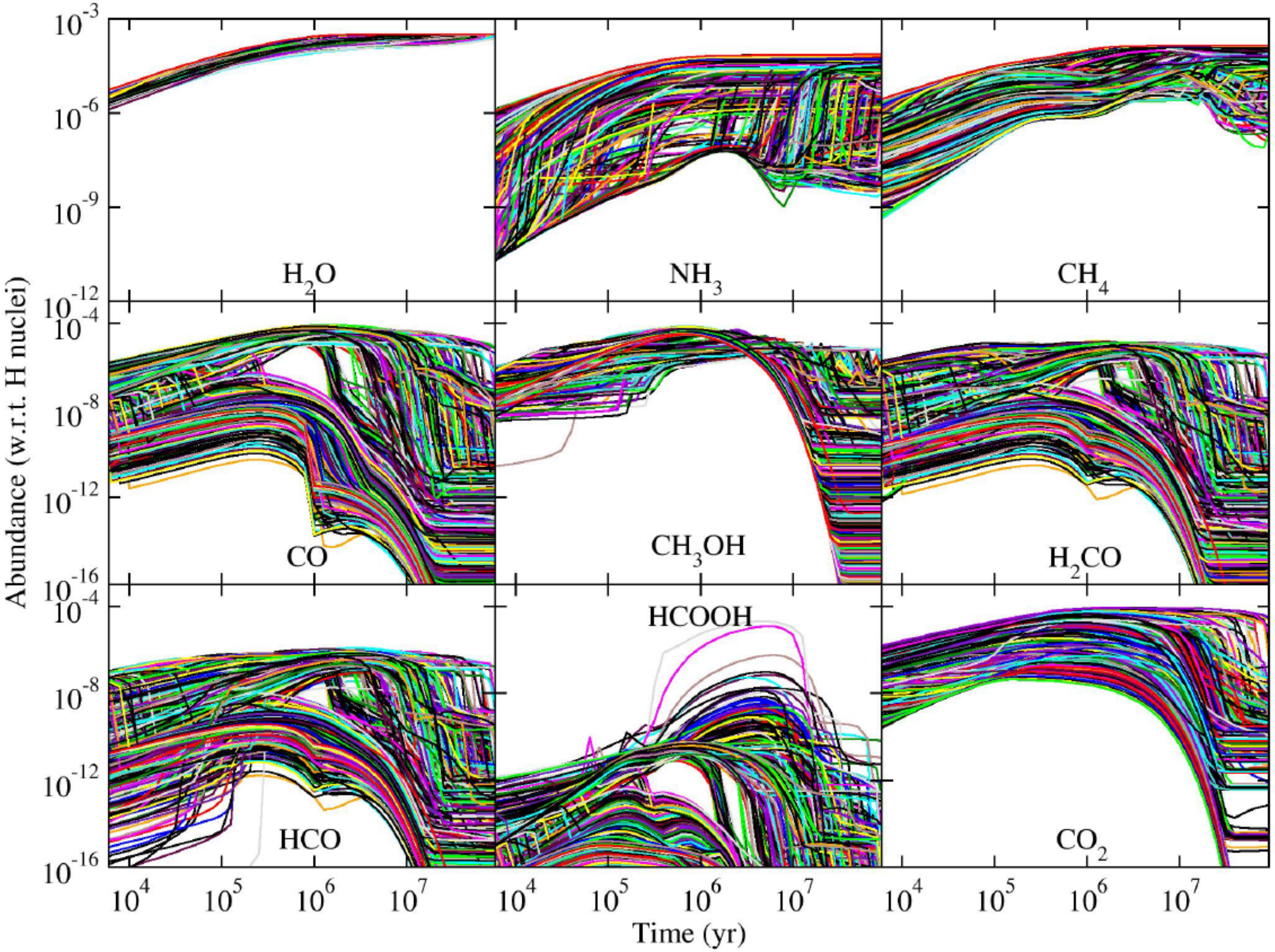

Ice abundance simulations in dark clouds *Penteado+2017*

Thermal Energy – Diffusion

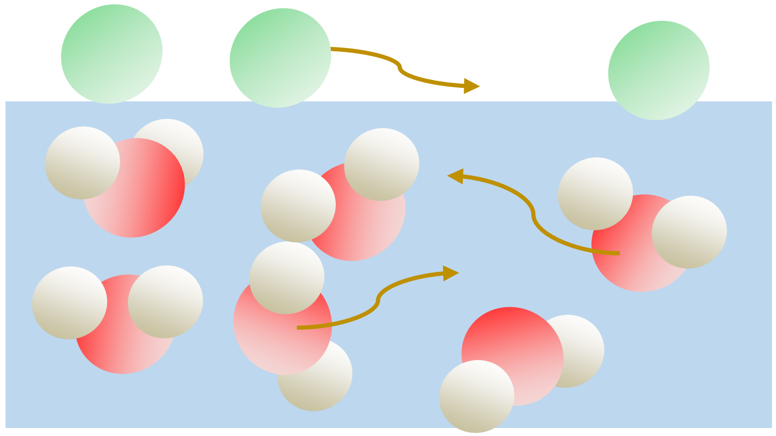

- limits the increase of molecular complexity
- understand the chemical evolution of molecular clouds

$$E_{diff} = f E_{ads} \; with \; f < 1$$

Surface E_{diff} < Bulk E_{diff}

Very scarce experiments

Thermal Energy- Diffusion

Furuya+ 2022

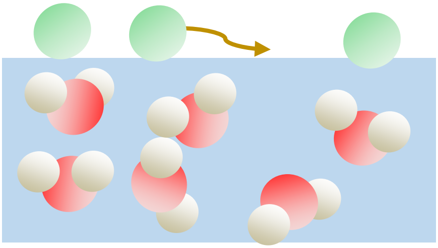

Direct experimental measure of surface E_{diff} by microscopy (Transmission Electron Microscopy)

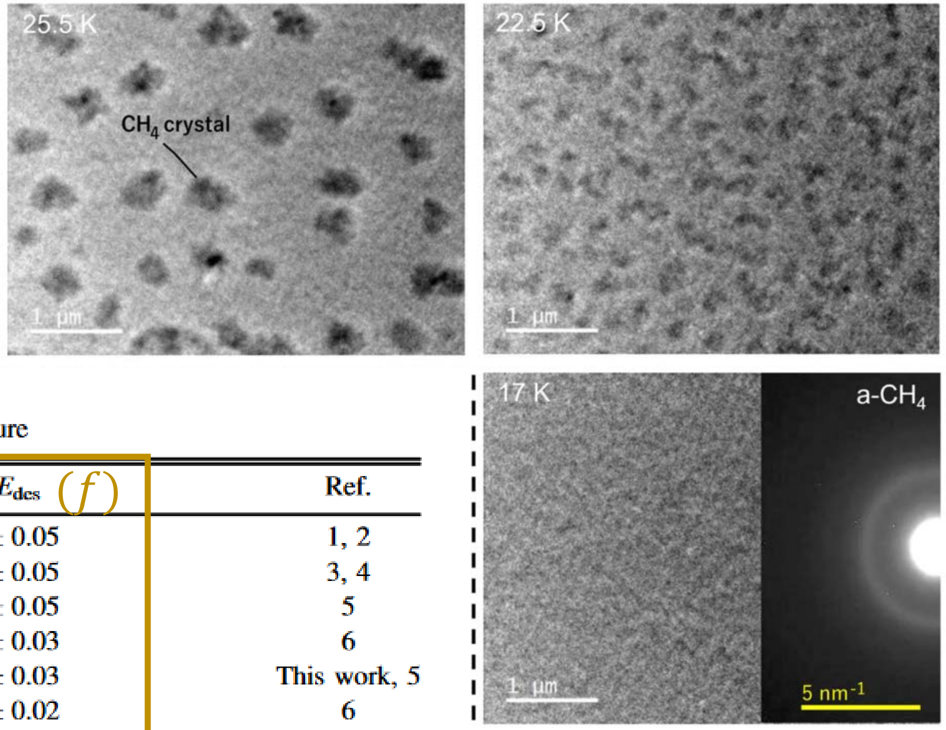

Table 1
Summary of Our Measured E_{sd} Values and Measured E_{des} Values Reported in the Literature

Molecule	Substrate	E_{sd} (K)	E_{des} (K)	E_{sd}/E_{des} (f)	Ref.
CO	p-ASW	350 ± 50	980	0.36 ± 0.05	1, 2
CO	c-ASW	200 ± 40	849 ± 55	0.24 ± 0.05	3, 4
			870	0.23 ± 0.05	5
			1420 ± 70	0.14 ± 0.03	6
CH_4	c-ASW	200 ± 30	1100	0.18 ± 0.03	This work, 5
			1370 ± 70	0.15 ± 0.02	6
H_2S	c-ASW	870 ± 130	2296 ± 90	0.38 ± 0.06	This work, 7
OCS	c-ASW	1690 ± 140	2325 ± 95	0.73 ± 0.06	This work, 7
CO_2	c-ASW	1500 ± 100	2256 ± 83	0.66 ± 0.04	1, 4
			2320	0.65 ± 0.04	5
CH_3CN	c-ASW	670 ± 210	3790 ± 130	0.18 ± 0.06	This work, 7
CH_3OH	c-ASW	920 ± 120	3820 ± 135	0.24 ± 0.03	This work, 7

Note. (2) He et al. (2016b), (1) Kouchi et al. (2020), (3) Kouchi et al. (2021b), (4) Noble et al. (2012), (5) He et al. (2016a), (6) Smith et al. (2016), (7) Penteado et al. (2017).

$0.2 < f < 0.7$ Surface E_{diff} depends on the surface species

Physico-chemical processes on/in ices

Thermal Energy

Thermal desorption

Diffusion

Non thermal Energy

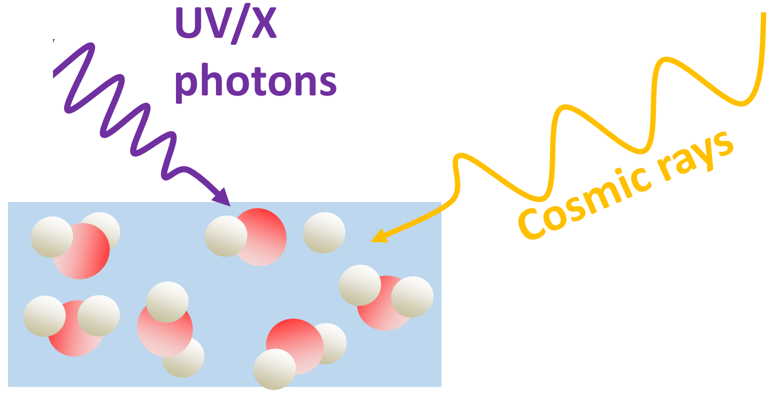

dissociation and chemistry

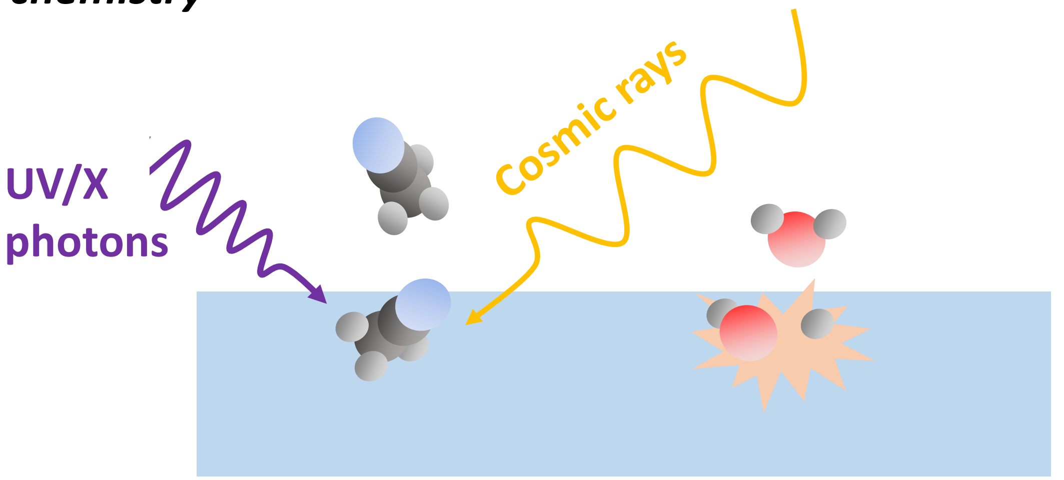

Desorption after photon/CR irradiation or chemical reaction

Minissale+ 2016

Non-thermal energy – Cosmic rays

- Cosmic Rays induce a change of the ice structure Dartois+ 2015

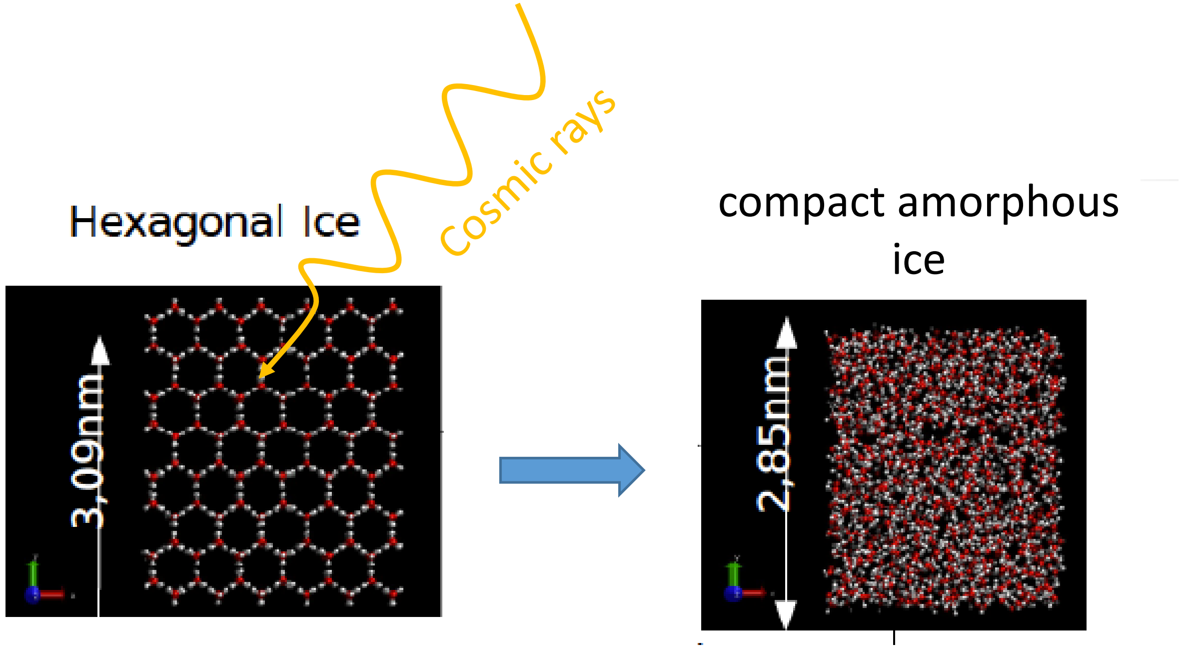

Tainter J Chem Phys 2014
Michoulier et al Phys chem chem phys 2018

- Cosmic Rays desorb molecules – H_2O from H_2O ices Dartois+ 2018 (Thickness dependence)

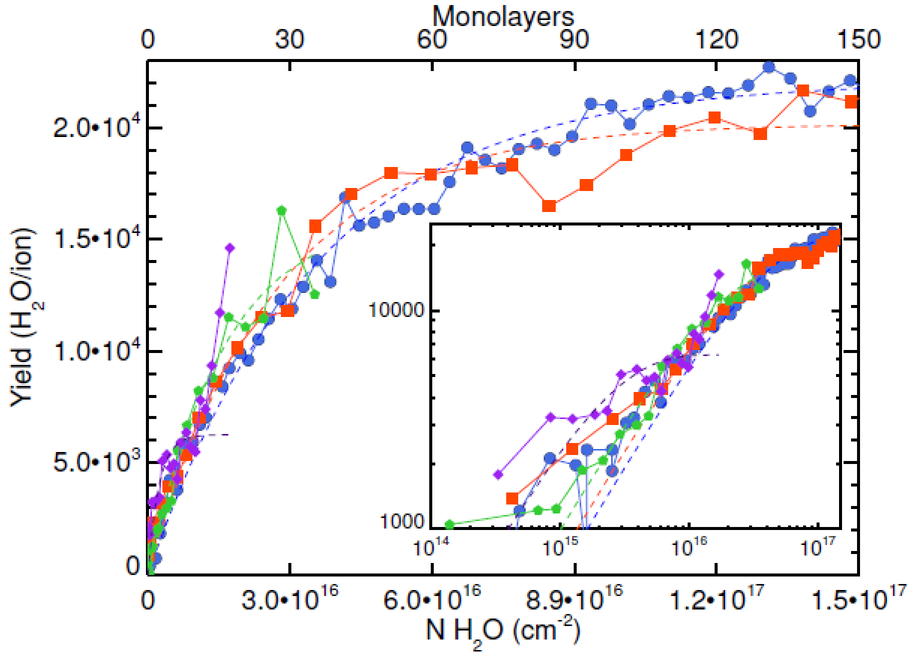

Fig. 5. Sputtering yield dependence calculated from the infrared spectral analysis, as a function of ice film column density. Dotted line correspond to a fit using equation 2. The colour coding is the same as for Fig. 3. The upper scale gives the corresponding number of ice monolayers assuming the ice density given in Table 1.

Dartois+ 2018

Astrochemical modeling of non thermal processes including cosmic rays : See Angèle Taillard's talk

Non-thermal energy – chemical reactions

Simplified results from Gutiérrez-Quintanilla+2021

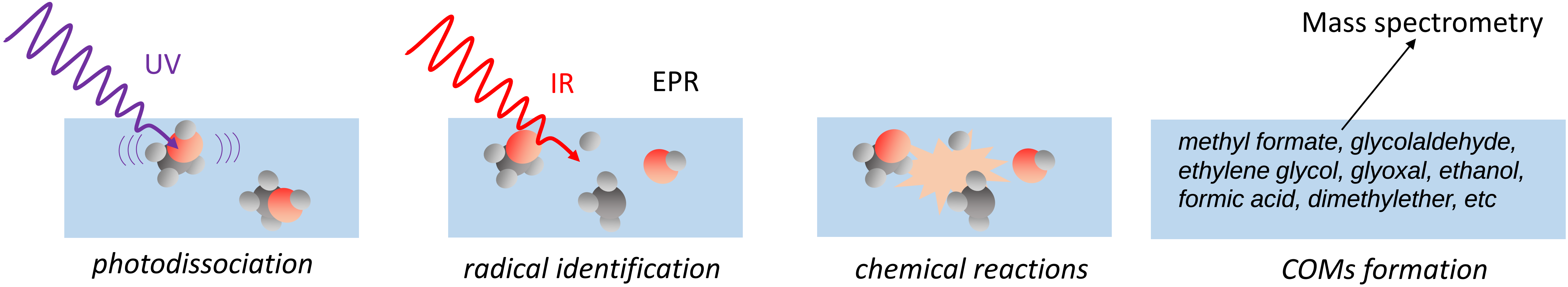

UV and X-ray photolysis of ices : See Céline Assadourian's poster

Non thermal energy - UV Photodesorption

The case of CH_3CN ice

SPICES (Surface Processes on ICES)
LERMA

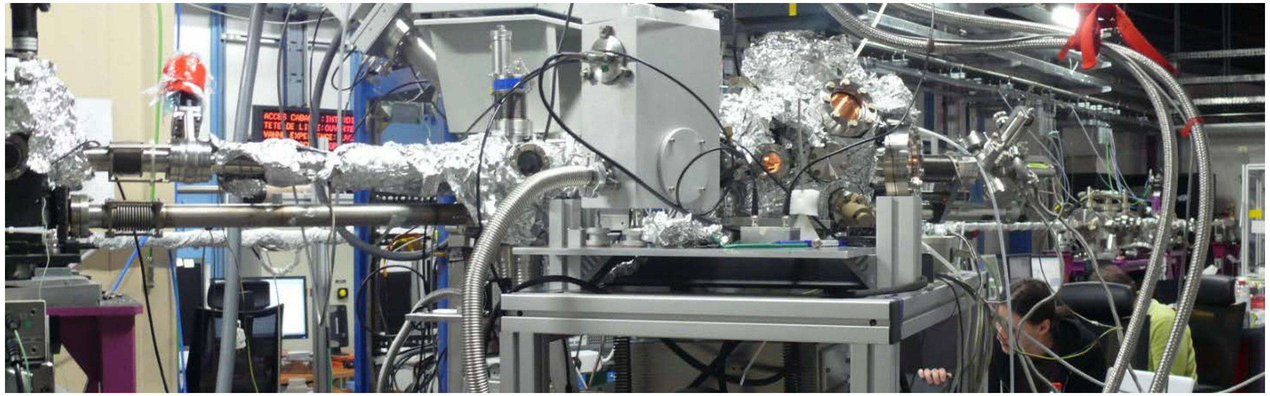

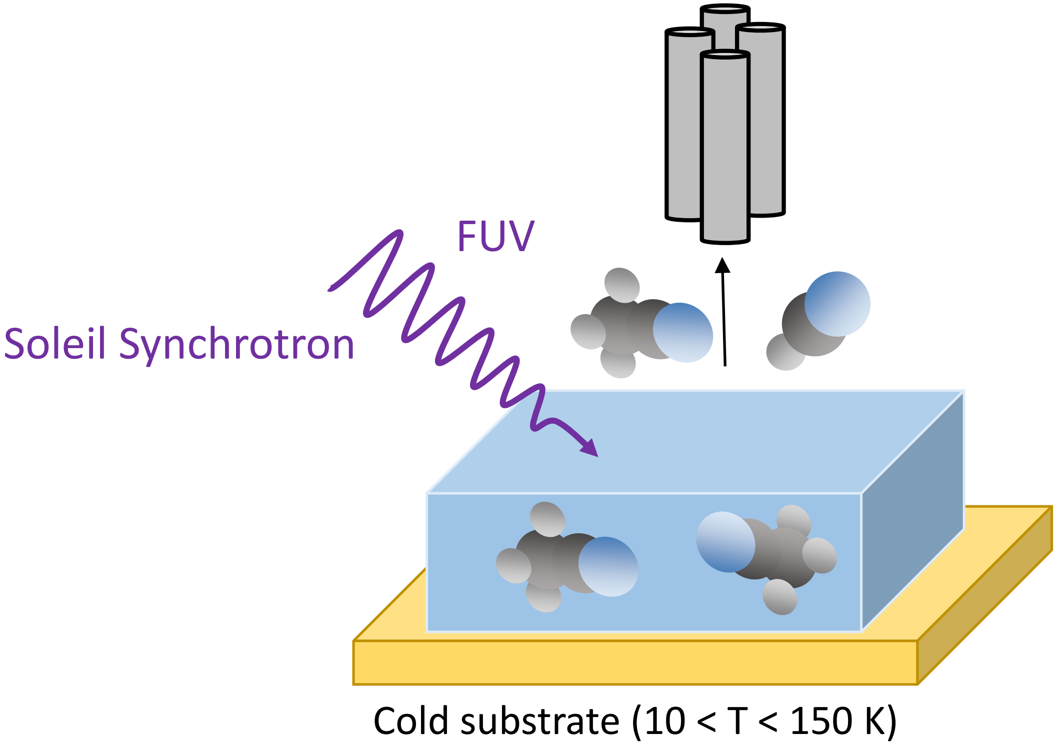

Basalgète+2021a

See Romain Basalgète talk for a description of the experiment

Non thermal energy - UV Photodesorption

The case of CH_3CN ice

Quantified experiments : how many molecules desorb

SPICES (Surface Processes on ICES)
LERMA

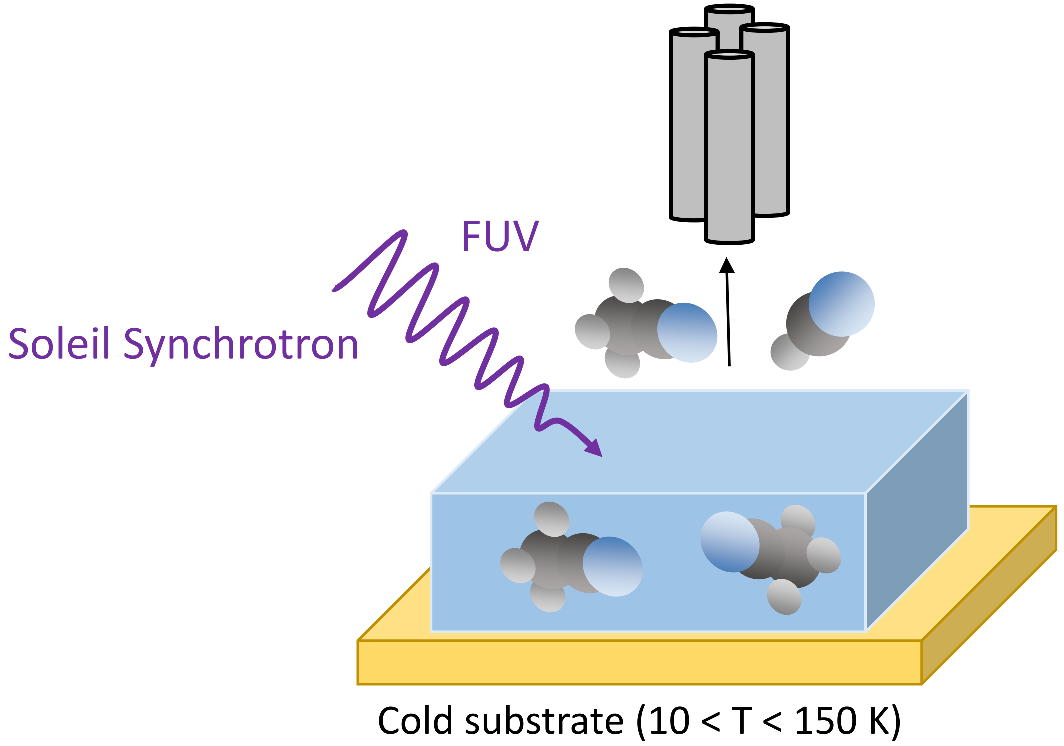

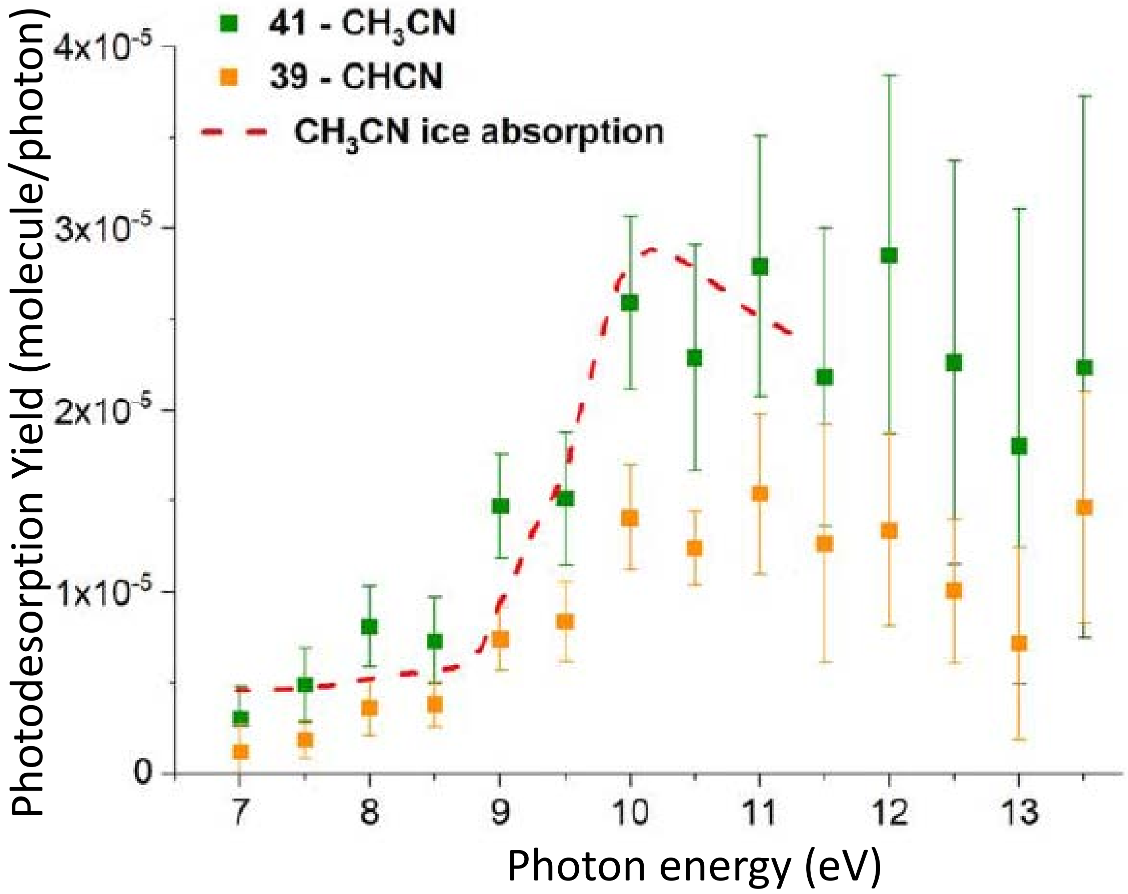

Basalgète+2021a

See Romain Basalgète talk for a description of the experiment

Non-thermal energy – UV Photodesorption Yields

The case of CH_3CN ice

Table 1
Astrophysical Photodesorption Yield ($\times 10^{-5}$ molecule photon^{-1}) Extrapolated from Our Experimental Results on Pure CH_3CN Ices at 15 K, for Different Astrophysical Environments

Photodesorbed Species	ISRF [(a)]	Dense Clouds [(b)] and Disks [(c)]
CH_3CN	0.67 ± 0.33	2.0 ± 1.0
CHCN	0.34 ± 0.17	1.0 ± 0.5
HCN	1.1 ± 0.6	3.3 ± 1.7
CN	0.60 ± 0.30	1.7 ± 0.9
CH_3	2.1 ± 1.0	6.5 ± 3.3

Basalgète+2021a

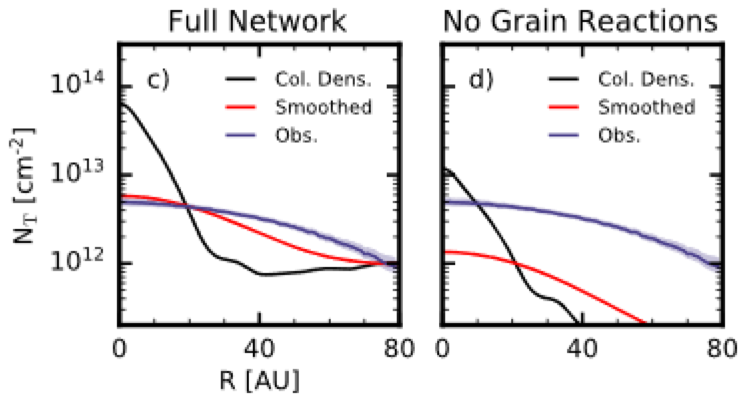

Loomis+2018

Figure 7. Panels (a, b): CH_3CN gas-phase abundances with grain-surface reactions turned on and off in the model, respectively. Temperature contours of 30 and 50 K are overlaid in black. Panels (c, d): CH_3CN gas-phase column densities for the abundance profiles shown in panels (a) and (b), respectively. Column density profiles smoothed with the synthesized beam are overplotted in red, and the observed column density profile from Figure 5 is overplotted in blue.

Processing of interstellar ices – More and more precise models

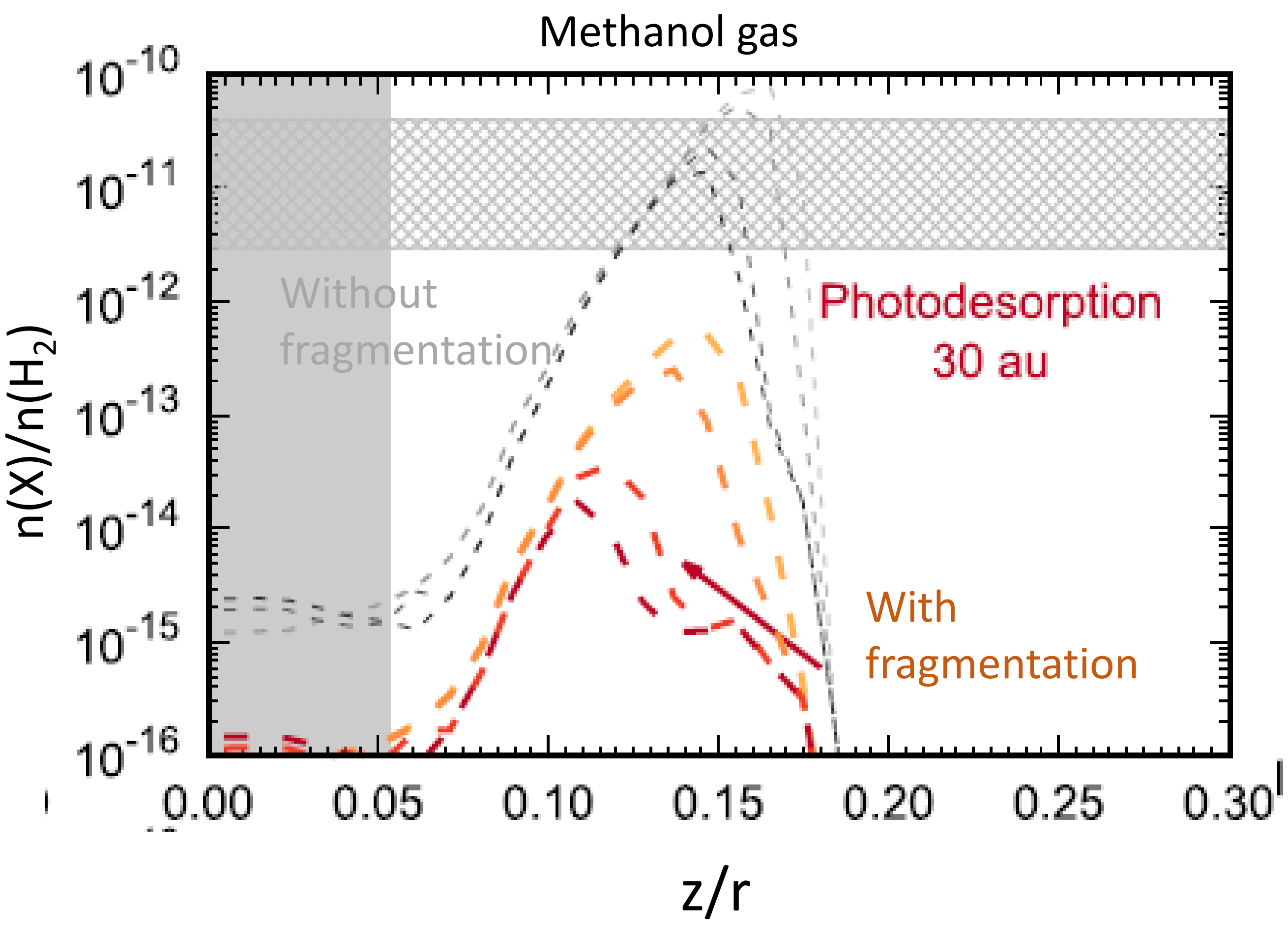

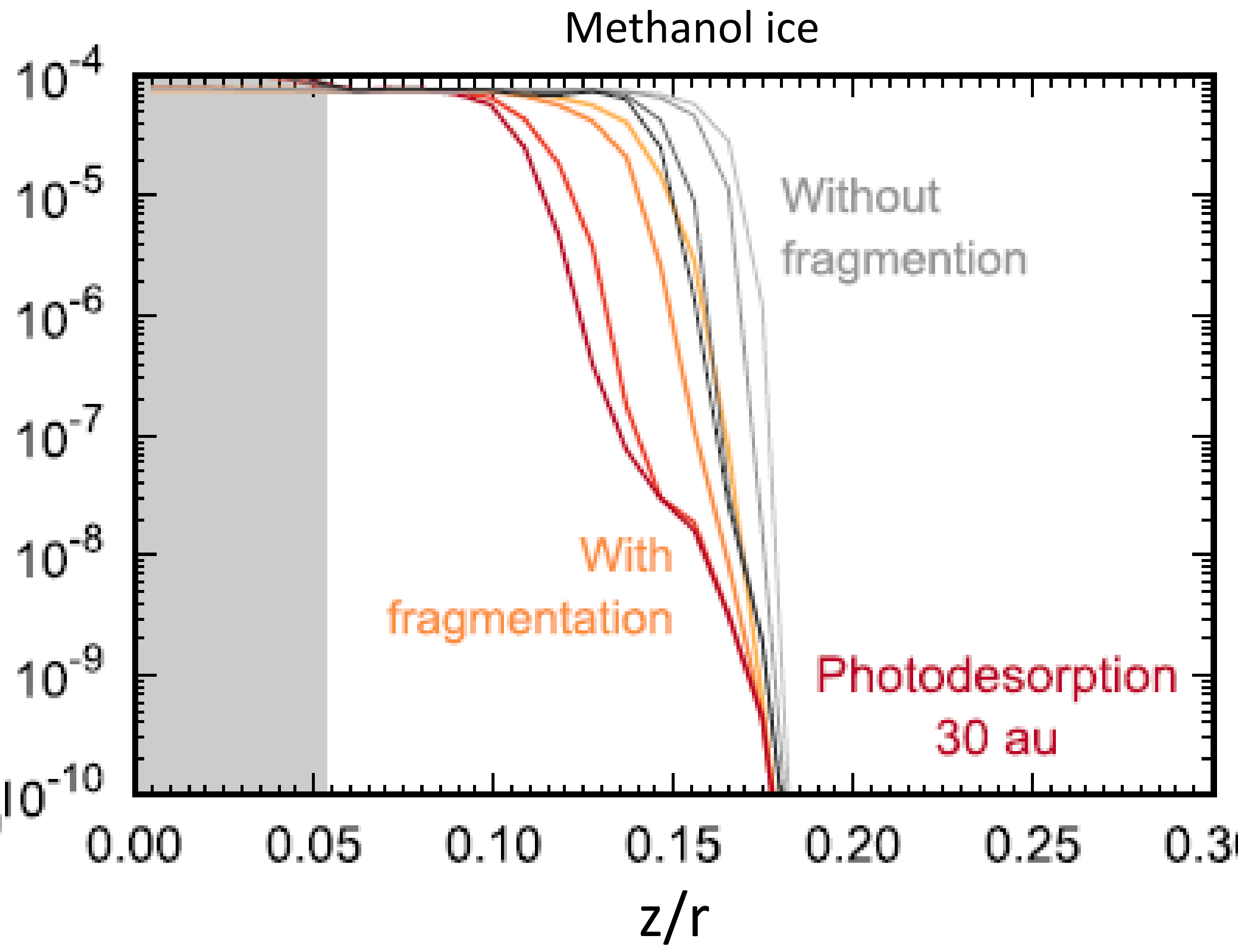

Ligterink+ 2018

Non-thermal energy – UV Photodesorption Yields

The case of CH_3CN ice

Table 1
Astrophysical Photodesorption Yield ($\times 10^{-5}$ molecule photon^{-1}) Extrapolated from Our Experimental Results on Pure CH_3CN Ices at 15 K, for Different Astrophysical Environments

Photodesorbed Species	ISRF [(a)]	Dense Clouds [(b)] and Disks [(c)]
CH_3CN	0.67 ± 0.33	2.0 ± 1.0
CHCN	0.34 ± 0.17	1.0 ± 0.5
HCN	1.1 ± 0.6	3.3 ± 1.7
CN	0.60 ± 0.30	1.7 ± 0.9
CH_3	2.1 ± 1.0	6.5 ± 3.3

Basalgète+2021a

CH_3CN is specific : photodesorption yields are approximatively the same when studying the pure ice or a mixed ice with CO
This is different from CH_3OH ice (10 times less desorption when mixing with CO) Bertin+2016

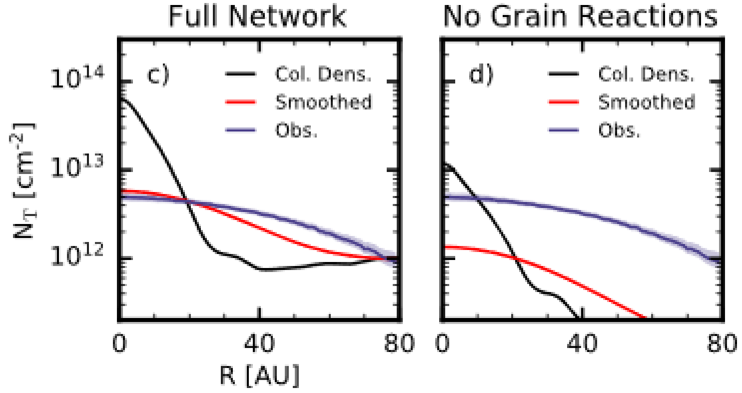

Loomis+2018

Figure 7. Panels (a, b): CH_3CN gas-phase abundances with grain-surface reactions turned on and off in the model, respectively. Temperature contours of 30 and 50 K are overlaid in black. Panels (c, d): CH_3CN gas-phase column densities for the abundance profiles shown in panels (a) and (b), respectively. Column density profiles smoothed with the synthesized beam are overplotted in red, and the observed column density profile from Figure 5 is overplotted in blue.

Non-thermal energy – UV Photodesorption Yields

What about X-rays instead of UV ? See Romain Basalgète talk !

Different ices studied with SPICES

Ice	Y (molecule/incident photon)	Y (molecule/absorbed photon)	Reference
CO	0.05	1	Fayolle+ 2011
N_2	0.03		Bertin+ 2013
NO	0.02		Dupuy+2017a
CO_2	10^{-3}	0.05	Fillion+2014
CH_4	$2\ 10^{-3}$	0.15	Dupuy+ 2017b
H_2O	$3\ 10^{-4}$	0.02	Fillion+ 2022
H_2CO	$4\ 10^{-4}$		Féraud+ 2019
CH_3CN	$3\ 10^{-5}$		Basalgète+ 2021a
CH_3OH	$< 10^{-6}$	$< 6\ 10^{-4}$	Bertin+ 2016
$C_xH_yO_z$	~~10^{-3}~~ Y		Towards a prediction of the photodesorption yields
	Default value used in the astrochemical models		

ANR PIXyES (PI : M. Bertin)

Non thermal energy – UV Photodesorption mechanisms

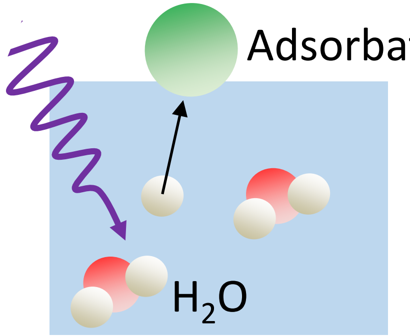

Photodesorption mechanisms are known for a few systems only

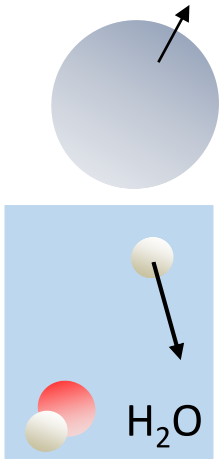

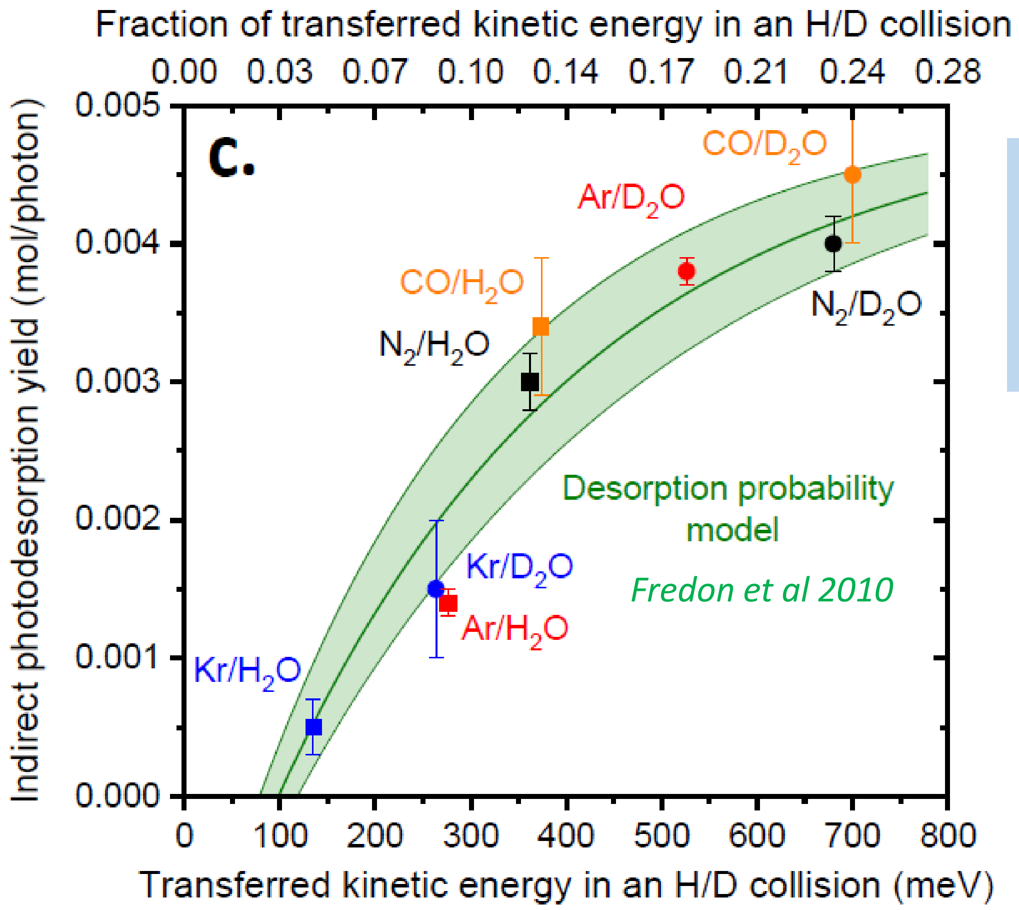

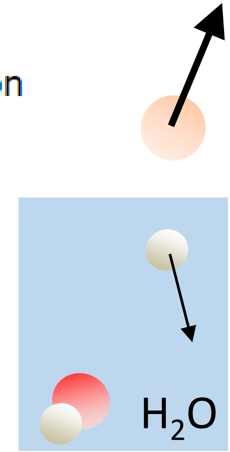

Model H_2O ice

Dupuy et al. 2021

Non thermal energy - UV Photodesorption mechanisms

<u>Pure H_2O ice</u>

Fillion et al. 2022

Photodissociation + photochemistry

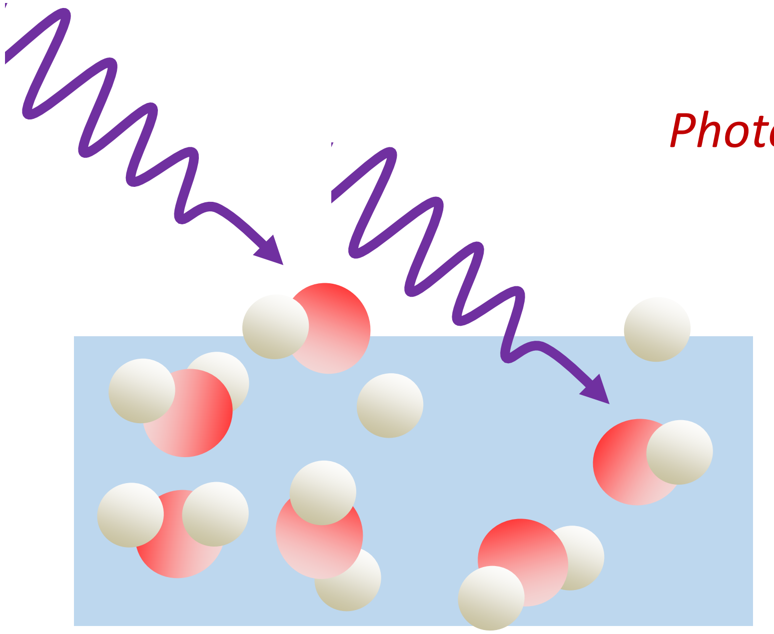

photodissociation

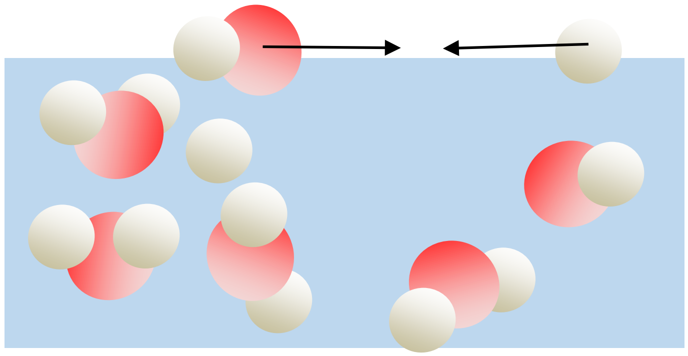

Exothermal reaction between fragments from different molecules

Unravelling the energy transfer in molecular ices (CO, N2) : See Samuel Del Fré's talk

Conclusion

- Complex processes when interstellar ices are irradiated (thermal or non-thermal energy)
- Improvements in **observations** push towards more and more precise and complete **experiments**, that provide inputs for astrochemical **models**

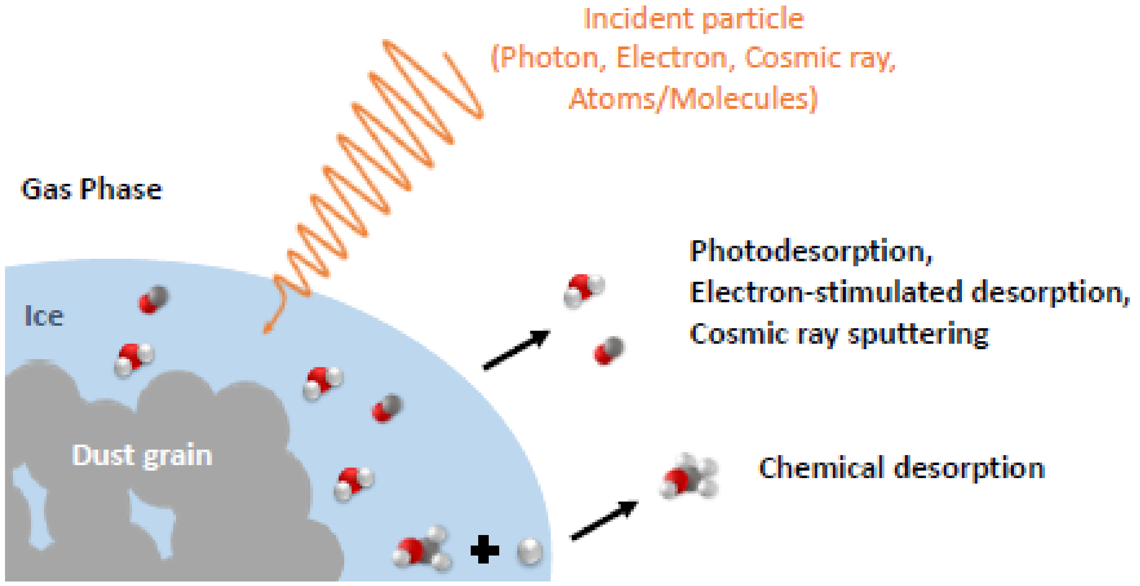

(Picture from R. Basalgète)